SLAC-PUB-11906
July 2006

CHARACTERIZATION OF THE PEP-II COLLIDING-BEAM PHASE SPACE BY THE BOOST METHOD*

M. Weaver†, Stanford Linear Accelerator Center, Stanford CA 94309, U.S.A.
W. Kozanecki, DAPNIA-SPP, CEA-Saclay, F91191 Gif-sur-Yvette, France
B. Viaud, Université de Montréal, Montréal, Québec, Canada H3C 3J7

Abstract

We present a novel approach to characterize the colliding-beam phase space at the interaction point of the energy-asymmetric PEP-II B-Factory. The method exploits the fact that the transverse-boost distribution of $e^+e^- \to \mu^+\mu^-$ events reconstructed in the *BABAR* detector reflects that of the colliding electrons and positrons. The mean boost direction, when combined with the measured orientation of the luminous ellipsoid, determines the e^+-e^- crossing angles. The average angular spread of the transverse boost vector provides an accurate measure of the angular divergence of the incoming high-energy beam, confirming the presence of a sizeable dynamic-β effect. The longitudinal and transverse dependence of the boost angular spread also allow to extract from the continuously-monitored distributions detailed information about the emittances and IP β-functions of both beams during high-luminosity operation.

INTRODUCTION

The *BABAR* detector is located at the interaction point (IP) of the PEP-II B Factory [1], where 9.0 GeV electrons from the high energy ring (HER) collide with 3.1 GeV positrons from the low energy ring (LER). The *BABAR* tracking system consists of a high-resolution silicon vertex tracker and a drift chamber [2]. The process $e^+e^- \to \mu^+\mu^-$ provides a detectable event rate of ≈ 4 Hz, and IP beam parameters imprint measurable signatures onto the spatial distributions of the μ-pair vertices [3, 4, 5]. The angular distribution of the muons, and its spatial variation, also carry information about the angular divergence of the beams at the IP, as well as about their crossing angle, emittances and β functions. In this paper, we first briefly outline the "boost" formalism, then describe the measurement technique, and finally present a characterization of the IP phase space under routine high-luminosity conditions.

The boost vector **B** is defined as the total three-momentum of the $\mu^+\mu^-$ pair. Its vertical angle $y'_{\rm B}$ is related to those of the parent electron and positron by

$$y'_{\rm B} = f_H y'_H - f_L y'_L \tag{1}$$

where $f_{H(L)}$ is the ratio of the HER (LER) energy to the difference in beam energies, and $y'_{H(L)}$ is the vertical angle of the colliding electron (positron). The same relation holds for the horizontal angles.

In the vertical direction, the bunch lengths are comparable to β^*. Assuming that the transverse shapes of both beams are approximately Gaussian, and neglecting dispersion and x-y coupling, the spread in vertical boost angle is given by

$$\sigma^2_{y'_{\rm B}} = \frac{f_H^2\epsilon^2_{y_H}}{\sigma^2_{y_H}} + \frac{f_L^2\epsilon^2_{y_L}}{\sigma^2_{y_L}} + \left(\frac{f_H\sigma_{yy'_H}}{\sigma^2_{y_H}} - \frac{f_L\sigma_{yy'_L}}{\sigma^2_{y_L}}\right)^2 \sigma^2_{y_{\mathcal{L}}} \tag{2}$$

with

$$\sigma^2_{y_H} = \epsilon_{y_H}\beta^*_{y_H} + (z - z_H)^2\,\frac{\epsilon_{y_H}}{\beta^*_{y_H}}$$
$$\sigma_{yy'_H} = (z - z_H)\,\frac{\epsilon_{y_H}}{\beta^*_{y_H}}$$
$$\sigma^{-2}_{y_{\mathcal{L}}} = \sigma^{-2}_{y_H} + \sigma^{-2}_{y_L}$$

Here $\epsilon_{y_{H(L)}}$ is the HER (LER) vertical emittance, $\beta^*_{y_{H(L)}}$ the corresponding IP β-function, z the longitudinal position of the $\mu^+\mu^-$ vertex, $z_{H(L)}$ that of the vertical waist, and $\sigma_{y_{\mathcal{L}}}$ the RMS vertical size of the luminous region.

In the horizontal plane, where β^* is considerably larger than the bunch lengths, the observable RMS boost angle is independent of z:

$$\sigma^2_{x'_{\rm B}} \approx \frac{f_H^2\epsilon_{x_H}}{\beta^*_{x_H}} + \frac{f_L^2\epsilon_{x_L}}{\beta^*_{x_L}} \tag{3}$$

Assuming similar ϵ_x/β^*_x ratios for the HER and LER, the spread in horizontal boost angle is dominated by the horizontal HER angular divergence $\sigma_{x'_H} = \sqrt{\epsilon_{x_H}/\beta^*_{x_H}}$.

The boost angles depend on the transverse and longitudinal position of the event vertex, in the reference frame defined by the axes of the luminous ellipsoid. In particular, the vertical vertex position and boost angle are related by

$$\left(\frac{dy'}{dy}\right)_{\rm B} = \frac{f_H(z - z_H)}{\beta^{*2}_{y_H} + (z - z_H)^2} - \frac{f_L(z - z_L)}{\beta^{*2}_{y_L} + (z - z_L)^2} \tag{4}$$

This relation is altered by (partially correlated) measurement errors on $y'_{\rm B}$ and on the vertex y-coordinate. Assuming Gaussian resolution functions, the observed $y - y'$ correlation obeys

$$\left(\frac{dy'}{dy}\right)_{\rm B,\ obs} = \frac{\sigma_{yy'_{\rm res}}}{\sigma^2_{y_{\mathcal{L}}} + \sigma^2_{y_{\rm res}}} + \left(\frac{f_H(z - z_H)}{\beta^{*2}_{y_H} + (z - z_H)^2} - \frac{f_L(z - z_L)}{\beta^{*2}_{y_L} + (z - z_L)^2}\right)\frac{\sigma^2_{y_{\mathcal{L}}}}{\sigma^2_{y_{\mathcal{L}}} + \sigma^2_{y_{\rm res}}} \tag{5}$$

where the vertical vertexing resolution $\sigma_{y_{\rm res}}$ and vertexing-trajectory correlation $\sigma_{yy'_{\rm res}}$ are extracted from the data.

* Work supported in part by DOE Contract DE-AC02-76SF00515
† weaver@slac.stanford.edu

MEASUREMENT TECHNIQUE

Because the high-energy $\mu^{\pm}$ tracks acquire only a small curvature in the solenoidal detector field, the magnitude of their momentum is poorly measured; the individual trajectory angles, however, are determined with great precision. We therefore measure the boost angles using the vector $\hat{n}$ normal to the $\mu^+\mu^-$ decay plane. This observable does not depend on track curvature measurements and is related to the $\mu^{\pm}$ momenta by

$$\hat{n} = \frac{\hat{p}_{\mu^+} \times \hat{p}_{\mu^-}}{\left\| \hat{p}_{\mu^+} \times \hat{p}_{\mu^-} \right\|} \tag{6}$$

The dip angle λ_n [6] and azimuth ϕ_n of this vector satisfy

$$\tan\lambda_n = -x'_{\rm B}\cos\phi_n - y'_{\rm B}\sin\phi_n \tag{7}$$

The typical single-event dip-angle resolution is 0.6 mrad.

The mean boost angles $\langle x'_{\rm B}\rangle$, $\langle y'_{\rm B}\rangle$ and their spread can thus be extracted from the azimuthal dependence of the mean dip angle $\langle\lambda_n\rangle$ and of its RMS spread σ_{λ_n}. The measured angular distribution of the vector $\hat{n}$ (Fig. 1a) illustrates the prediction of Eq. 7; in particular, the nominal 20 mrad horizontal angle between the PEP-II beam axis and that of the *BABAR* solenoid is clearly visible. For this data sample, the RMS angular spread of the boost direction is $\sigma_{x'_{\rm B}} = 1.11$ ($\sigma_{y'_{\rm B}} = 0.73$) mrad (Fig. 1b).

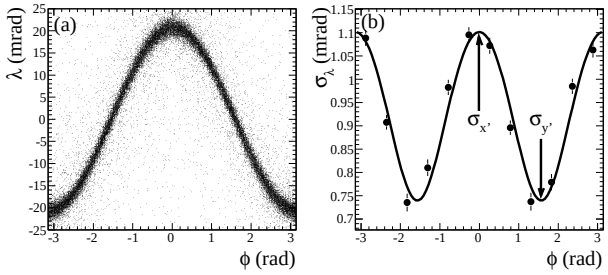

Figure 1: (a) Observed μ-pair distribution in the λ_n - ϕ_n plane, in the *BABAR* reference frame. (b) Azimuthal dependence of the resolution-corrected angular spread σ_{λ_n}.

IP PHASE-SPACE CHARACTERIZATION

Fig. 2a displays the long-term history of the mean horizontal boost angle $\langle x'_{\rm B}\rangle$. Also shown is the horizontal tilt of the luminous ellipsoid, computed as the beam–size-weighted average of the e^+ and e^- angles:

$$\langle x'\rangle_{\mathcal{L}} = \left\langle \frac{dx}{dz} \right\rangle_{\mathcal{L}} = \frac{\langle x'_H\rangle\,\sigma^2_{x_L} + \langle x'_L\rangle\,\sigma^2_{x_H}}{\sigma^2_{x_L} + \sigma^2_{x_H}} \tag{8}$$

Their difference provides an estimate of the full horizontal e^+-e^- crossing angle θ_c under the assumption that the x-sizes of the two beams are equal. If $|z| \ll \beta^*_x$,

$$\langle x'_{\rm B}\rangle - \langle x'\rangle_{\mathcal{L}} = \frac{1}{2}\left(f_H + f_L + \frac{\sigma^2_{x_L} - \sigma^2_{x_H}}{\sigma^2_{x_H} + \sigma^2_{x_L}}\right)\langle x'_H - x'_L\rangle \overset{\sigma_{xH}=\sigma_{xL}}{\longrightarrow} \frac{f_H + f_L}{2}\langle x'_H - x'_L\rangle \approx 1.03\ \langle x'_H - x'_L\rangle \tag{9}$$

The resulting ~ 0.3 mrad crossing angle (Fig. 2b) is consistent with the optimum θ_c value determined using orbit monitors during dedicated beam-beam experiments [7].

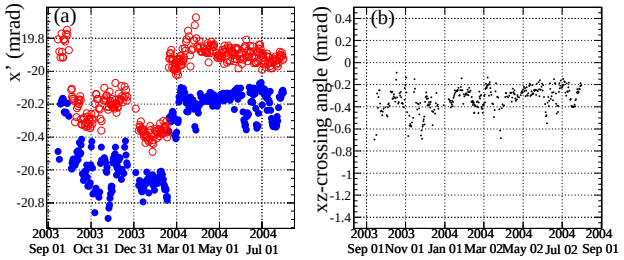

Figure 2: (a) History of the mean horizontal boost angle (blue closed circles) and the horizontal luminous tilt (red open circles). (b) Horizontal crossing-angle history.

The e^- angular divergence, integrated over the luminous region, can be estimated directly from the angular spread of the boost vector, applying a small ($\sim$ 6%) correction for the LER contribution (Eqs. 2, 3). The five-year history of the horizontal luminous size [4] and e^- angular divergence, reconstructed from archived *BABAR* data, is presented in Fig. 3. The sharp reduction in $\sigma_{x_{\mathcal{L}}}$ and increase in $\sigma_{x'_H}$ reflect the onset of the significant dynamic-β enhancement that occurred (dotted line) when the tunes of both rings were moved very close to the half-integer, resulting also in an appreciable luminosity increase. A more detailed discussion of horizontal phase-space characterization is presented in Ref. [8].

A first set of constraints on the waist positions, vertical emittances and IP β-functions is supplied by the z-dependence of the boost angular spread (Eq. 2). One such measurement of $\sigma_{x'_{\rm B}}$, $\sigma_{y'_{\rm B}}$ in slices of longitudinal vertex position is illustrated in Fig. 4. The z-dependence of the boost–angle-position correlation (Fig. 5), which exhibits a different functional dependence on the same beam parameters (Eq. 5), provides complementary information.

The measurement and fit procedure were validated with a GEANT4 Monte Carlo simulation of $e^+e^- \to \mu^+\mu^-$ events in the *BABAR* detector. Fits to the $\sigma_{y'_{\rm B}}(z)$ and $(dy'/dy)_{\rm B,\ obs}(z)$ distributions, with as free parameters independent HER and LER vertical emittances, a common β^*_y, a common vertical-waist location, and the resolution parameter $\sigma_{yy'_{\rm res}}$, were carried out using *BABAR* data spanning several months of operation (Fig. 6). Using only the spread information allows a precise estimate of the HER vertical emittance, leaving that of the LER poorly determined. Including the $y - y'_{\rm B}$ correlation significantly improves the statistical precision, but at the cost of systematic anticorrelated shifts in ϵ_{y_H} and ϵ_{y_L}. Preliminary studies

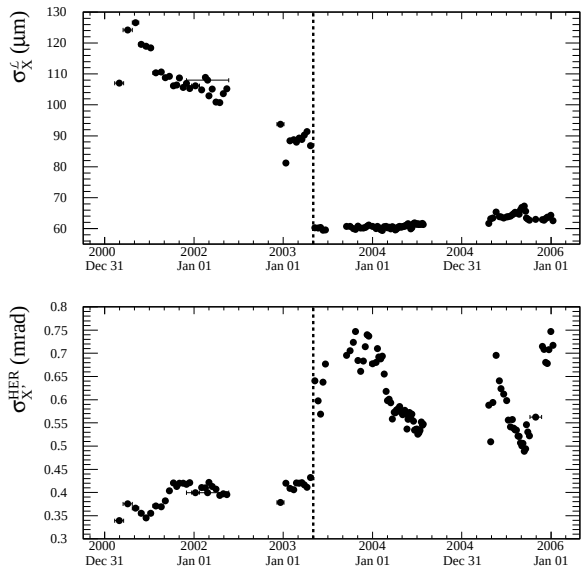

Figure 3: Long-term evolution of $\sigma_{x_{\mathcal{L}}}$ and $\sigma_{x'_H}$.

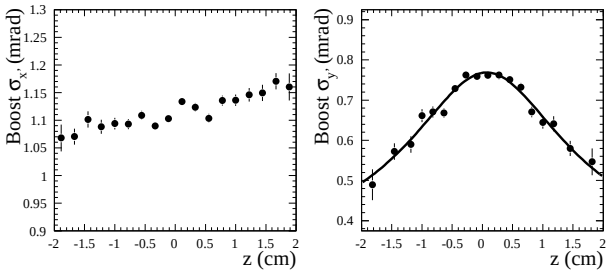

Figure 4: Measured z-dependence of the horizontal and vertical boost angular spread. The slope of $\sigma_{x'_{\mathrm{B}}}$ (left) indicates that the average x-waist is offset by a few cm towards positive z with respect to the average collision point. The curvature of $\sigma_{y'_{\mathrm{B}}}$ (right) reflects the fact that $\beta_y^* \ll \beta_x^*$, and its amplitude is related to $(\epsilon/\beta^*)_{y_{L,H}}$.

suggest that x- y coupling terms in the IP $e^{\pm}$ beam matrices may be responsible for such inconsistencies when analyzing the data in terms of the uncoupled formalism assumed throughout this paper. For instance, simulations using fully coupled-lattice functions measured by resonant excitation predict similarly correlated shifts in fitted vertical emittances for certain combinations of true $e^{\pm}$ eigenemittances. Similar shifts are also predicted in the $\beta^*_{y_{L,H}}$ measurements by this and other luminous-region methods [4] when the fully coupled-lattice functions are considered.

SUMMARY

Analysis of the transverse-boost distribution of $\mu^+\mu^-$ pairs reconstructed in *BABAR* provides detailed information about the emittances and lattice functions of the two beams at the PEP-II IP. A strategy to combine these results with independent measurements extracted from the 3-D luminosity distribution and from beam profile monitors in the two rings, is presented in Ref. [8].

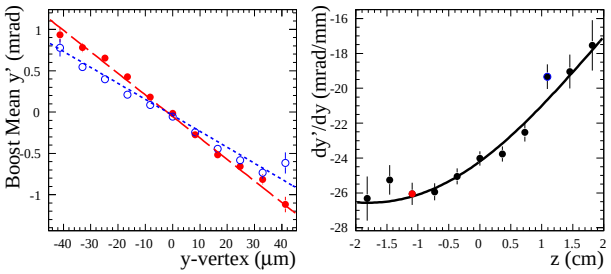

Figure 5: Correlation between vertical boost angle and vertex position. Left: y'_{B} *vs.* y at $z = -1$ (red circles, dashed) and $z = +1$ cm (open blue circles, dotted). The lines are fits to the data. Right: fitted $\left(\frac{dy'}{dy}\right)_{\mathrm{B}}$ slope *vs.* z. The sample is restricted to quasi-horizontal μ tracks, resulting in an almost Gaussian vertexing resolution with $\sigma_{y_{\mathrm{res}}} = 19\,\mu$m.

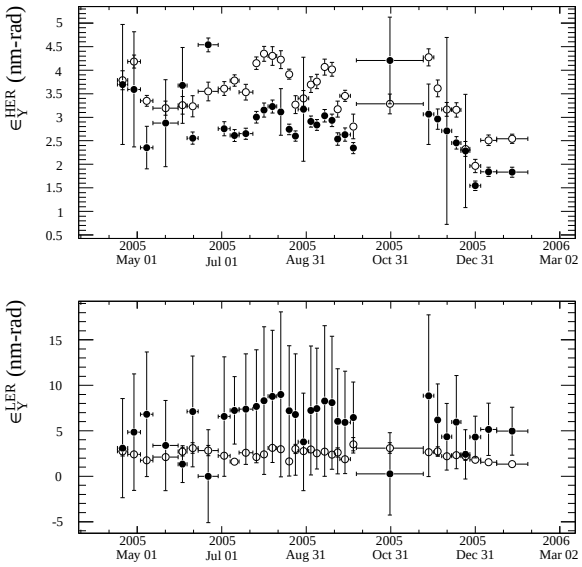

Figure 6: History of the vertical emittance in the HER (top) and LER (bottom), extracted from fits to $\sigma_{y'_{\mathrm{B}}}$ only (closed circles), or from combined fits to $\sigma_{y'_{\mathrm{B}}}$ and $(dy'/dy)_{\mathrm{B,\,obs}}$ (open circles).

REFERENCES

[1] J. Seeman *et al.*, EPAC-2006-MOPLS045.

[2] B. Aubert *et al.* [*BABAR* Collaboration], "The *BABAR* Detector", Nucl. Instrum. Meth. A **479**, 1 (2002).

[3] D. Cinabro *et al.*, PAC-2001-TPPH152.

[4] B. F. Viaud *et al.*, SLAC-PUB-11900 (2006).

[5] J. Thompson *et al.*, SLAC-PUB-11222 (2005).

[6] $\lambda = \pi/2 - \theta$, with θ being the polar angle.

[7] W. Kozanecki *et al.*, SLAC-PUB-11216 (2005).

[8] A. Bevan *et al.*, SLAC-PUB-11904 (2006).